Brief Report

DOI: 10.5582/bst.2023.01214

Genome-wide identification of mammalian cell-cycle invariant and mitotic-specific macroH2A1 domains

Le Zhang[1,2,3,§], Bishan Ye[2,3,§], Zeqian Xu[2,3,§], Xinhui Li[2,3,*], D.M. Czajkowsky[2,3], Zhifeng Shao[1,2,3,*]

[1] State Key Laboratory of Systems Medicine for Cancer, Shanghai Jiao Tong University, Shanghai, China;
[2] Bio-ID Center, Shanghai Jiao Tong University, Shanghai, China;
[3] School of Biomedical Engineering, Shanghai Jiao Tong University, Shanghai, China.

SUMMARY The histone variant macroH2A has been found to play important regulatory roles in genomic processes, especially in regulating transcriptomes. However, whether macroH2A nucleosomes are retained on mitotic chromosomes to enable maintenance of cell-specific transcriptomes is not known. Here, examining mouse embryonic fibroblast cells (NIH-3T3) with native chromatin immunoprecipitation and sequencing (nChIP-seq), we show that the overwhelming majority (~90%) of macroH2A1 domains identified at the G1/S stage are indeed stably retained on mitotic chromosomes. Unexpectedly though, we also find that there are a number of macroH2A domains that are specific for either mitotic or G1/S cells. Notably, more than 7,000 interphase expressed genes flanked by macroH2A1 domains are loaded with macroH2A1 nucleosomes on the mitotic chromosome to form extended domains. Overall, these results reveal that, while the majority of macroH2A1 domains are indeed faithfully transmitted through the mitotic chromosomes, there is a previously unknown cell-cycle dependent exchange of macroH2A1 nucleosomes at numerous genomic loci, indicating the existence of molecular machineries for this dynamically regulated process. We anticipate that these findings will prove to be essential for the integrity of mitotic progression and the maintenance of cellular identity.

Keywords Histone variant macroH2A1, cell cycle, mitotic chromosomes, nChIP-seq

1. Introduction

The most basic structural and regulatory unit of eukaryotic chromatin is the nucleosome, consisting of an octamer of four core histone proteins, H2A, H2B, H3 and H4 or their variants. The locations of nucleosomes within the genome, their composition, as well as the modifications to the core histones are all well-known to play important roles in a wide range of genomic processes (*1,2*). Among the known histone variants, macroH2A is markedly distinguished, both structurally and functionally (*3*). Structurally, macroH2A is roughly three-fold larger than the canonical H2A histone owing to the presence of a unique 30 kDa macro-domain at its C-terminus (*4*). Functionally, previous work has found that macroH2A forms broad domains spanning many kilobases which are distributed over the entire genome (*4,5*) and often associated with transcriptional silencing with colocalization with heterochromatin domains marked by H3K27me3 and H3K9me3 in some cases (*6-8*). As a result, macroH2A is thought to contribute significantly to the means by which the cell produces its characteristic transcriptome, and thus its identity.

As such, it may be expected that the locations of macroH2A within the genome are retained through mitosis in order to ensure the maintenance of the phenotypical properties within the daughter cells, similar to what is believed for the histone modifications (*9-12*). However, to date, direct examinations of the nucleosomal compositions of the mitotic chromosomes, and in particular the macroH2A content, has not been reported. In fact, owing to the significant compaction of the chromatin during mitosis, it may be that macroH2A is removed from the chromatin prior to mitosis, owing to its large macrodomain, to facilitate a maximal extent of packaging of the genome to ensure its faithful transmission to daughter cells (*13,14*). Indeed, there has been recent work describing mechanisms by which macroH2A can be dynamically exchanged within interphase (*15*), although whether these, or other mechanisms, are functional in a cell cycle dependent manner is presently unknown.

To address these questions, we performed genome-wide profiling of macroH2A1 on both mitotic chromosomes and G1/S chromatin in mouse embryonic fibroblast cells (NIH-3T3) using native chromatin immunoprecipitation and sequencing (nChIP-seq). We found that a large fraction of macroH2A1 domains is indeed invariant during the cell cycle. However, mitotic chromosomes also contain substantially more macroH2A1 domains when compared with that of G1/S chromatin, indicating that macroH2A1 must be reloaded before and unloaded after mitosis at specifically defined genomic regions. Many of these mitotic-specific domains overlap with genes that are expressed in the interphase. Thus, while the majority of macroH2A1 domains are preserved in the mitotic chromosomes, there are also numerous specifically defined genomic regions that exhibit changes in macroH2A1 nucleosomes in a cell cycle dependent manner, whose functional consequences may also prove to be critical for the proper progression of mitosis and the maintenance of phenotypic properties.

2. Materials and Methods

2.1. Cell culture and cell cycle synchronization

Mouse embryonic fibroblast NIH-3T3 cells were cultured in DMEM (GIBCO, Carlsbad, CA, USA) supplemented with 10% FBS (GIBCO, Carlsbad, CA, USA) and 1% Pen/Strep (GIBCO, Carlsbad, CA, USA) at 37℃, 5% CO_2.

To obtain G1/S synchronized NIH-3T3 cells, cells were cultured with starvation treatment (DMEM with 0.5% FBS and 1% Pen/Strep) for 48 h, followed with fresh medium containing 1% Aphidicolin (Abcam, Cambridge, MA, USA) for 18 h before collection. With this procedure, about 97% of the collected cells were G1/S cells based on FACS (Fluorescence-Activated Cell Sorting) analysis (Supplementary Figure S1A, *http://www.biosciencetrends.com/action/getSupplementalData.php?ID=168*). To obtain mitotic cells, cells in culture reached 70-80% confluence were treated with colcemid (100 ng/mL, Sigma-Aldrich, St. Louis, MO, USA) for 12 h, and mitotic cells were shaken-off and collected for mitotic chromosome purification. The purity of the collected mitotic cells was about 77% by FACS analysis (supplementary Figure S1B, *http://www.biosciencetrends.com/action/getSupplementalData.php?ID=168*).

2.2. Mitotic chromosome purification and mononucleosome preparation

To minimize the contamination of interphase cells, highly purified mitotic chromosomes were obtained using the protocol described previously (*16*) with modifications (see SI for details). Briefly, the collected mitotic cells were centrifuged and resuspended in a hypotonic solution (75 mM KCl) for 30 min at 37℃. The cells were then suspended in the polyamine buffer (PA buffer) (*17*) developed to protect the integrity of the chromosomes and were homogenized on ice. Large debris were removed with centrifugation at 190× *g* at 4°C and the supernatant was filtered by 10 μm and 5 μm filter membranes sequentially. The mitotic chromosomes were collected by centrifugation and the pellet was resuspended in the MNase (Micrococcal Nuclease) buffer containing spermidine and spermine, as well as a protease inhibitor cocktail. Under such conditions, the mitotic chromosome morphology remained intact as examined with fluorescence microscopy with DAPI (Vector Laboratories, Burlingame, CA, USA) staining (supplementary Figure S1C, *http://www.biosciencetrends.com/action/getSupplementalData.php?ID=168*). These mitotic chromosomes were then digested with MNase (3,000 gel units/mL, NEB, Ipswich, MA, USA) at 4°C overnight and terminated with 20 mM EDTA. The supernatant containing mononucleosomes was collected after centrifugation at 10,000× *g* at 4°C. As shown in Figure S1D (*http://www.biosciencetrends.com/action/getSupplementalData.php?ID=168*), the chromosomes were fully reduced to mononucleosomes with the characteristic 146 bp length DNA. Under our conditions, the nucleosomal DNA was well protected and no further loss of DNA was found with additional MNase digestion beyond this point. These mononucleosomes were used for immunoprecipitation.

2.3. Mononucleosome preparation from G1/S chromatin

G1/S synchronized 3T3 cells were collected after trypsin digestion and washed with ice-cold PBS before resuspended in the MNase buffer supplemented with 0.5% NP-40 for membrane permeabilization. These G1/S cells were digested with MNase (2,000 gel units/mL) at 4°C overnight. After this step, the G1/S chromatin was mostly reduced to mononucleosomes with the characteristic 146 bp length DNA (supplementary Figure S1E, *http://www.biosciencetrends.com/action/getSupplementalData.php?ID=168*). These mononucleosomes were ready for immunoprecipitation.

2.4. Native chromatin immunoprecipitation and sequencing

Native ChIP of macroH2A1 was performed with the collected mononucleosomes of either G1/S or mitotic preparations in the immunoprecipitation (IP) buffer (*18*), both with two biological replicates. Rabbit anti-macroH2A1 antibody (ab37624 that recognizes both 1.1 and 1.2 isoforms; Abcam, Cambridge, MA, USA) was first loaded onto protein A+G coated magnetic beads (16-663, Millipore, Billerica, MA, USA) following the

recommended procedure by the supplier. These beads were then mixed with the mononucleosome solution and incubated overnight at 4°C under constant rotation. The recovered magnetic beads were washed and the bound nucleosomes were eluted as recommended. Input mononucleosomes (used for normalization) or the ChIPed macroH2A1 nucleosomes were first incubated with 100 μg/mL RNase A (Invitrogen, Carlsbad, CA, USA) to remove RNA contamination followed with 1% SDS and 200 μg/mL Proteinase K (Invitrogen, Carlsbad, CA, USA) incubation overnight at 56°C. The DNA in these samples were purified with phenol chloroform and ethanol precipitation. Sequencing libraries were prepared from ~1 ng of DNA per sample using the NEBNext® Ultra™ II DNA Library Prep Kit (E7645S, NEB, Ipswich, MA, USA) and sequencing was performed with Illumina® NovaSeq 6000.

2.5. ChIP-seq data processing

Quality control and adapter trimming were performed with TrimGalore. The reads with Q ≥ 20 were retained for further analysis. Qualified reads were aligned to the mouse reference genome (UCSC, mm10) using Bowtie2 (*19*). Samtools (*20*) was used to remove the reads mapped to blacklist regions, unknown chromosome segments, as well as those unmappable reads and the reads mapped to mitochondria genome. The mapped reads were de-duplicated using Sambamba markdup (*21*) and the unique reads were retained. Pearson correlation between the unique reads was calculated using multiBamsummary with 1 kb bins and visualized with the Deeptools (*22*) of plotCorrelation. Well correlated replicates were then combined for macroH2A1 domain analysis after normalization by the control (input nucleosome DNA) by normR (*23*).

To identify macroH2A1 enriched domains, we divided the reference genome into 1 kb bins. In each bin, the midpoint of each mapped fragment was counted, the normalized ratio of macroH2A1 ChIP/Input were calculated as the enrichment-score using normR (*23*). Fisher's exact test was used to identify significantly enriched macroH2A1 bins and adjacent ones were merged into enriched domains. Using exportR (*23*), the coordinates of enriched domains were created and displayed on Integrative Genomics Viewer (*24*).

H3K27me3 and H3K9me3 ChIP-seq data for NIH-3T3 cells were downloaded from Gene Expression Omnibus (GEO) (accession number: GSE73432) and re-analyzed using the same procedure for macroH2A1.

To identify macroH2A1 associated genes, BedTools (*25*) was used to align macroH2A1 enriched domains onto annotated genes including non-coding genes. ComputeMatrix and plotProfile options of the DeepTools (*22*) were used to visualize macroH2A1 coverage on different types of genes.

2.6. RNA data analysis

RNA-seq data of unsynchronized NIH-3T3 cells were downloaded from GEO (accession number: GSE152724). TrimGalore (*26*) was used to perform quality control and adapter trimming, and reads with Q ≥ 20 were retained and mapped onto the UCSC mm10 reference genome using Hisat2 (*27*) and uniquely mapped reads were retained. Count table was generated using featureCounts and calculated into FPKM (Fragments Per Kilobase of transcript per Million fragments mapped). Reads coverage files were generated using Deeptools (*22*).

3. Results and Discussion

3.1. macroH2A1 is broadly distributed across the genome in both G1/S and mitotic cells

To gain insight into the degree to which macroH2A is maintained on the chromatin during the cell cycle, we profiled the genomic distribution of macroH2A1 in mouse embryonic fibroblast cells (NIH-3T3) synchronized at G1/S phase and at metaphase (supplementary Figure S2, *http://www.biosciencetrends.com/action/getSupplementalData.php?ID=168*) using magnetic beads-based ChIP-seq of native chromatin. With this method, the DNA that is protected by the macroH2A1-containing nucleosomes is recovered and sequenced. For the mitotic cells, we sequenced two biological replicates with about 113 million and 93 million uniquely mapped pair-end reads after removal of duplicates, while for the G1/S cells, we sequenced two replicates with 28 million and 42 million uniquely mapped reads (supplementary Table S1, *http://www.biosciencetrends.com/action/getSupplementalData.php?ID=168*). The replicates were highly reproducible under both conditions (Pearson correlation: $R^2 > 0.97$) (Figure 1A), and so were combined to improve the reliability of the subsequent analysis.

We first calculated the macroH2A1 enrichment using 1 kb bins over the entire genome. Using a threshold FDR (False Discovery Rate) of 0.1, we found that 64.3% of the mappable genome in the G1/S cells was enriched for macroH2A1-containing nucleosomes (supplementary Figure S3A, *http://www.biosciencetrends.com/action/getSupplementalData.php?ID=168*), in agreement with previous findings (*6*). By contrast, we found that 75.6% of the genome in the mitotic cells was enriched with macroH2A1 nucleosomes (supplementary Figure S3A, Table S2, *http://www.biosciencetrends.com/action/getSupplementalData.php?ID=168*). Figure 1B is a graphic representation of the macroH2A1 domains on chromosome 19 for both G1/S and mitotic cells. These results demonstrate that a substantial fraction of the genome (> 10%) must be selectively loaded

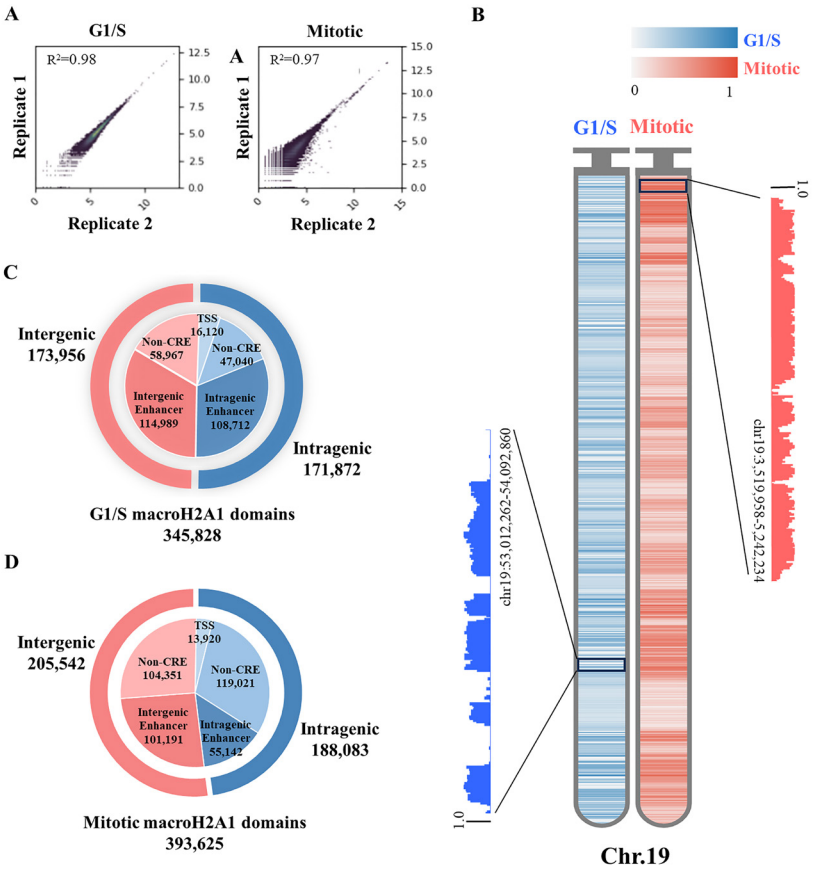

Figure 1. macroH2A1 enriched domains are broadly distributed across the entire genome in both G1/S chromatin and mitotic chromosomes. (**A**) The replicates of the ChIP-seq data are highly consistent for both G1/S and mitotic cells. (**B**) Graphic demonstration of macroH2A1 enrichment distribution on chromosome 19 for G1/S and mitotic cells. The enrichment score is color coded as indicated. Distribution of macroH2A1 domains with known functional elements on the genome: (**C**) G1/S cells; (**D**) mitotic cells. Overall, mitotic cells have more macroH2A1 enriched domains than that of G1/S cells (393,625 vs. 345,828). The median size of these domains is similar under both conditions.

with macroH2A1 nucleosomes before mitosis which must also be removed subsequently in the G1 phase after mitosis. Thus, these data clearly indicate that the nucleosome composition of the chromatin is more dynamic during the cell cycle than presently believed.

Since many of the macroH2A1-enriched bins were neighboring each other, we merged adjacent bins into extended domains for both G1/S and mitotic cells. In this way, we found that there are ~14% more macroH2A domains in mitotic cells over the G1/S cells (393,625 and 345,828, respectively) (Figures 1C and 1D), although both exhibit a median size of 10 kb (supplementary Table S2, *http://www.biosciencetrends.com/action/getSupplementalData.php?ID=168*). The normalized average reads density of these enriched domains is 5.8 (± 0.8) and 6.6 (± 1.0) CPM (counts per million) per kb for G1/S and mitotic cells, respectively, indicating that the average density of the macroH2A1 containing nucleosomes in these enriched domains is comparable across the genome under both conditions.

3.2. macroH2A1 domains in G1/S cells are significantly enriched at silenced genes

Since macroH2A1 is known to play critical roles in gene regulation (*4,6,28*), we examined the relationship of the macroH2A1-enriched domains with the expression status of the associated genes in the G1/S cells. We found that about 50% (173,956) of the domains were located in the intergenic regions, with the remaining domains localized within the annotated genes. For the latter, 16,120 domains overlapped putative TSS (Transcription Start Site) regions, while 155,752 were found within the gene bodies (supplementary Table S3, *http://www.biosciencetrends.com/action/getSupplementalData.php?ID=168*). Overall, the bodies of 18,679 annotated genes were substantially covered with macroH2A1 domains (Figure 2A). As expected (*28*), 90% of these genes (16,811) were significantly down-regulated or silenced (FPKM < 1), which constitutes about 40% of all silenced genes in this cell. Interestingly, it should be noted that for the remaining 10% of the genes (1,868), nearly half (784) were expressed at levels above the median of all expressed genes (median FPKM = 9.14). Although the molecular basis for these exceptions is not clear, it may be of interest that a fraction of these "abnormally" expressed genes are non-coding RNA genes or pseudogenes. The macroH2A1 domains located at TSS regions corresponded to 7,254 annotated genes that were expressed at a low level (median FPKM = 1.2), similar to previous observations in other cell types (*29*). For the intergenic macroH2A1 domains, about 66% (114,989) were found at annotated enhancers and 99,407 enhancers were fully covered by the macroH2A1 domains. Together with the intragenic

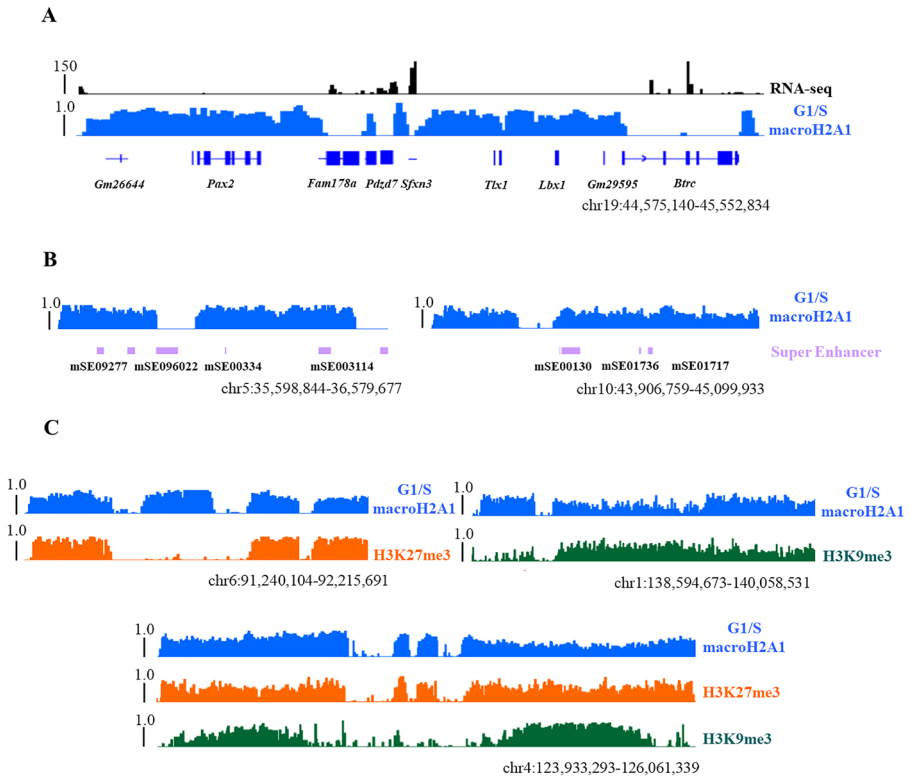

Figure 2. Representative examples to demonstrate the various localization of macroH2A1 domains. (**A**) Gene bodies fully covered by macroH2A1 are sufficient to inhibit expression and the expressed genes are mostly devoid of macroH2A1 occupancy. (**B**) Some (super) enhancers are extensively covered by macroH2A1 domains, presumably also silenced. (**C**) Examples of co-localization of macroH2A1 domains with heterochromatin domains demarcated by either H3K27me3 (upper penal, left) or H3K9me3 (upper panel, right) or both (lower panel).

enhancers that were also fully covered with macroH2A1 domains, we found that 1,276,213 putative enhancers (Figure 2B) were presumably silenced by macroH2A1, corresponding to 59% of all putative enhancers noted in the ENCODE database (based on all cell-types characterized to date) (*30*).

Since it has been reported that macroH2A was also preferentially localized in heterochromatin domains (*4*), we next examined colocalization of the macroH2A1 domains with the domains demarcated by the canonical heterochromatin markers, H3K27me3 and H3K9me3 (*6,7*). Using published data for this cell type with the same criteria for macroH2A1 domain assignment, we found that 41,008 out of 345,828 macroH2A1 domains colocalized with H3K27me3 domains (median size of 2 kb) and 90,336 with H3K9me3 domains (median size of 1 kb). Together, 124,064 macroH2A1 domains (36%) co-localized with either or both of the heterochromatic H3 marked domains (Figure 2C and supplementary Table S3, *http://www.biosciencetrends.com/action/getSupplementalData.php?ID=168*). Interestingly, among the silenced genes (16,811) associated with macroH2A1, less than half (47%) were found in these co-localized domains where macroH2A1 and heterochromatin could play redundant functions. It is perhaps more intriguing to note that more macroH2A1 silenced genes (8,937) were not found in the heterochromatin domains, suggesting that macroH2A1 is not simply redundant with heterochromatin as proposed previously (*6*) and could be sufficient for gene silencing.

Thus, overall, our results, as well as those in other studies (*28,30*), unequivocally implicate an important role of macroH2A1 domains in the silencing of a large number of genes and enhancers. Therefore, it follows that their retainment at specific genomic loci, particularly those important to the phenotype, must be reliably regulated, especially during cell proliferation.

3.3 Mitotic chromosome-specific macroH2A1 domains are abundant and loci-specific

To determine the extent to which the macroH2A domains were retained during the cell cycle, we compared the domains identified in the G1/S cells with those present in the mitotic cells. We found that the overwhelming majority of the G1/S macroH2A1 domains, nearly 90% (305,595 out of 345,828), were also present in the mitotic chromosomes in terms of both location and size, demonstrating that macroH2A1 domains are indeed largely conserved through the cell cycle (Supplementary Figure S3B, *http://www.biosciencetrends.com/action/getSupplementalData.php?ID=168*). These fully conserved macroH2A1 domains included 58% of the genes with substantial gene body coverage in the G1/S cells, and 70%

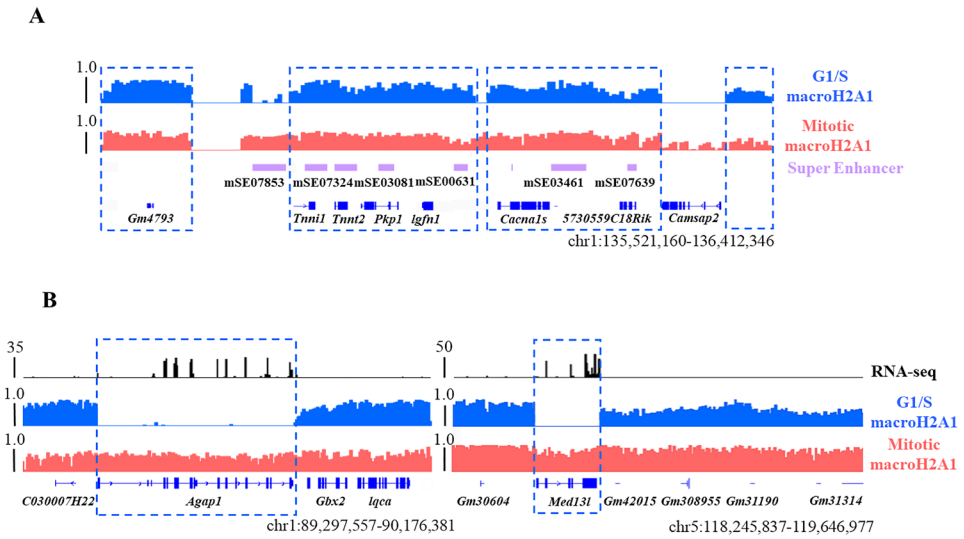

Figure 3. Comparison of macroH2A1 enriched domains in G1/S and mitotic cells. (**A**) Representative example of conserved macroH2A1 domains between G1/S and mitotic cells (highlighted by dashed blue boxes). (**B**) Two examples to demonstrate that some of the highly expressed genes with flanking macroH2A1 domains in G1/S cells are loaded by macroH2A1 nucleosomes before mitosis to form extended and continuous macroH2A1 domains.

of the TSS localized domains, as well as 86% of the enhancers (Figure 3A and supplementary Table S4, *http://www.biosciencetrends.com/action/getSupplementalData.php?ID=168*). This high level of transmission of the macroH2A1 domains through mitotic chromosomes suggests that macroH2A1 might also be a constituent of mitotic bookmarkers in order to ensure phenotype identity, similar to histone modifications that are stably transmitted through cell division (*11*). However, we also found that a fraction (40,233) of G1/S macroH2A1 domains was not present on the mitotic chromosomes (Supplementary Figure S3B, *http://www.biosciencetrends.com/action/getSupplementalData.php?ID=168*), including 744 out of the 16,811 macroH2A1 silenced genes and 23,422 of the 1,276,213 macroH2A1 covered enhancers (supplementary Table S4, *http://www.biosciencetrends.com/action/getSupplementalData.php?ID=168*). The functional significance underlying the removal of these macroH2A1 nucleosomes from the chromatin before entry into mitosis is not understood, although it is clear that they are restored after mitosis.

More unexpectedly though is the finding that there are 88,030 macroH2A1 domains that are specific to the mitotic chromosome (supplementary Figure S3B, *http://www.biosciencetrends.com/action/getSupplementalData.php?ID=168*), indicating that these macroH2A1 domains were established before entering mitosis. Among these mitotic-specific macroH2A1 domains, 60% (52,828) were found to overlap substantially with 7,715 gene bodies (supplementary Figure S3C, *http://www.biosciencetrends.com/action/getSupplementalData.php?ID=168*) and the remaining were distributed in the intergenic regions, including 10,873 enhancers. Moreover, the genes that overlap these mitotic-specific domains were all well-expressed in the G1/S cells, and include some that were highly expressed, such as 64 histone genes (such as H2ac8 and H2bc3), 42 housekeeping genes and other important genes such as the ubiquitin gene, *Ubc*. A clearly notable feature of the genes specifically loaded with macroH2A1 in the mitotic cell was that they were flanked on both sides by macroH2A1 domains in the G1/S cells, so that extended macroH2A1 domains were formed on the mitotic chromosome (Figure 3B). We speculate that the formation of these extended domains in mitotic cells is necessary to fully silence the transcription in these regions on the mitotic chromosome (*31*), the failure of which could lead to aneuploidy (*32*), in order to ensure a proper packing of the chromatin, although further studies are certainly required to determine their functioning. Nonetheless, these results clearly indicate that there must be molecular machinery in the cell that not only performs loading and removal of macroH2A1 nucleosomes during the cell cycle but must also targets select loci robustly. In this regard, the ability to exchange macroH2A nucleosomes in the interphase was already shown with modified fibroblasts (*15*), but whether this mechanism also plays a role in the cell cycle-dependent macroH2A1 exchange remains to be examined.

In conclusion, we have performed the first genome-wide profiling of macroH2A1 domains at different stages of the cell cycle. We found that macroH2A1 domains are widely distributed over the entire genome in both G1/S and mitotic cells, with nearly 90% of the domains stably retained. We speculate that this retainment may be a critical means of maintaining proper cellular functioning and thus, *in vivo*, is important especially within stem

cells and progenitor cells (that is, the major cycling cells in any organism) to prevent transformation into pathological phenotypes. However, we also found that for a subset of the expressed genes in G1/S cells that are demarcated by flanking macroH2A1 domains, macroH2A1 nucleosomes are loaded before mitosis to form extended macroH2A1 domains on the mitotic chromosomes. Our data also indicate that macroH2A1 coverage over the gene body alone (that is, without co-localizing heterochromatin) might be sufficient for transcriptional repression in 21% of all silenced genes in the G1/S cells. Together with macroH2A1 domains localized at the enhancers, our results support the notion that macroH2A1 could play important epigenetic functions in phenotype maintenance.

Acknowledgements

We thank Yixin Liu for useful discussions and experimental assistance.

Funding: This work was supported by grants from the National Key R&D Program of China (2020YFA0908100), the National Natural Science Foundation of China (31971151, 81627801, 81972909) and the K.C. Wong Education Foundation (H.K.).

Conflict of Interest: The authors have no conflicts of interest to disclose.

Data accessibility

The data presented in this study are uploaded on the NCBI GEO (*https://www.ncbi.nlm.nih.gov/geo/*) under accession number GSE234016.

References

1. Cutter AR, Hayes JJ. A brief review of nucleosome structure. FEBS Lett. 2015; 589:2914-2922.
2. Zhang Y, Sun Z, Jia J, Du T, Zhang N, Tang Y, Fang Y, Fang D. Overview of histone modification. Adv Exp Med Biol. 2021; 1283:1-16.
3. Biterge B, Schneider R. Histone variants: key players of chromatin. Cell Tissue Res. 2014; 356:457-466.
4. Sun Z, Bernstein E. Histone variant macroH2A: from chromatin deposition to molecular function. Essays Biochem. 2019; 63:59-74.
5. Changolkar LN, Singh G, Cui K, Berletch JB, Zhao K, Disteche CM, Pehrson JR. Genome-wide distribution of macroH2A1 histone variants in mouse liver chromatin. Mol Cell Biol. 2010; 30:5473-5483.
6. Gaspar-Maia A, Qadeer ZA, Hasson D, Ratnakumar K, Leu NA, Leroy G, Liu S, Costanzi C, Valle-Garcia D, Schaniel C, Lemischka I, Garcia B, Pehrson JR, Bernstein E. MacroH2A histone variants act as a barrier upon reprogramming towards pluripotency. Nat Commun. 2013; 4:1565.
7. Douet J, Corujo D, Malinverni R, Renauld J, Sansoni V, Posavec Marjanovic M, Cantarino N, Valero V, Mongelard F, Bouvet P, Imhof A, Thiry M, Buschbeck M. MacroH2A histone variants maintain nuclear organization and heterochromatin architecture. J Cell Sci. 2017; 130:1570-1582.
8. Changolkar LN, Pehrson JR. macroH2A1 histone variants are depleted on active genes but concentrated on the inactive X chromosome. Mol Cell Biol. 2006; 26:4410-4420.
9. Wang C, Zhu B, Xiong J. Recruitment and reinforcement: Maintaining epigenetic silencing. Sci China Life Sci. 2018; 61:515-522.
10. Kim JE. Bookmarking by histone methylation ensures chromosomal integrity during mitosis. Arch Pharm Res. 2019; 42:466-480.
11. Reinberg D, Vales LD. Chromatin domains rich in inheritance. Science. 2018; 361:33-34.
12. Halsall JA, Andrews S, Krueger F, Rutledge CE, Ficz G, Reik W, Turner BM. Histone modifications form a cell-type-specific chromosomal bar code that persists through the cell cycle. Sci Rep. 2021; 11:3009.
13. Chakravarthy S, Gundimella SK, Caron C, Perche PY, Pehrson JR, Khochbin S, Luger K. Structural characterization of the histone variant macroH2A. Mol Cell Biol. 2005; 25:7616-7624.
14. Kozlowski M, Corujo D, Hothorn M, *et al*. MacroH2A histone variants limit chromatin plasticity through two distinct mechanisms. EMBO Rep. 2018; 19:e44445.
15. Sun Z, Filipescu D, Andrade J, Gaspar-Maia A, Ueberheide B, Bernstein E. Transcription-associated histone pruning demarcates macroH2A chromatin domains. Nat Struct Mol Biol. 2018; 25:958-970.
16. Yusuf M, Parmar N, Bhella GK, Robinson IK. A simple filtration technique for obtaining purified human chromosomes in suspension. Biotechniques. 2014; 56:257-261.
17. Gasser S, Laemmli U. Improved methods for the isolation of individual and clustered mitotic chromosomes. Exp Cell Res. 1987; 173:85-98.
18. Brind'Amour J, Liu S, Hudson M, Chen C, Karimi MM, Lorincz MC. An ultra-low-input native ChIP-seq protocol for genome-wide profiling of rare cell populations. Nat Commun. 2015; 6:6033.
19. Langmead B, Salzberg SL. Fast gapped-read alignment with Bowtie 2. Nat Methods. 2012; 9:357-359.
20. Danecek P, Bonfield JK, Liddle J, Marshall J, Ohan V, Pollard MO, Whitwham A, Keane T, McCarthy SA, Davies RM, Li H. Twelve years of SAMtools and BCFtools. Gigascience. 2021; 10:giab008.
21. Tarasov A, Vilella AJ, Cuppen E, Nijman IJ, Prins P. Sambamba: Fast processing of NGS alignment formats. Bioinformatics. 2015; 31:2032-2034.
22. Ramirez F, Ryan DP, Gruning B, Bhardwaj V, Kilpert F, Richter AS, Heyne S, Dundar F, Manke T. deepTools2: A next generation web server for deep-sequencing data analysis. Nucleic Acids Res. 2016; 44:W160-165.
23. Helmuth J, Li N, Arrigoni L, Gianmoena K, Cadenas C, Gasparoni G, Sinha A, Rosenstiel P, Walter J, Hengstler JG, Manke T, Chung H-R. normR: Regime enrichment calling for ChIP-seq data. BioRxiv. 2016; 082263.
24. Robinson JT, Thorvaldsdottir H, Turner D, Mesirov JP. igv.js: An embeddable JavaScript implementation of the Integrative Genomics Viewer (IGV). Bioinformatics. 2023; 39:btac830.
25. Quinlan AR, Hall IM. BEDTools: A flexible suite of

utilities for comparing genomic features. Bioinformatics. 2010; 26:841-842.
26. Github. FelixKrueger/TrimGalore. *https://github.com/FelixKrueger/TrimGalore* (accessd April 10, 2008).
27. Kim D, Langmead B, Salzberg SL. HISAT: A fast spliced aligner with low memory requirements. Nat Methods. 2015; 12:357-360.
28. Gamble MJ, Frizzell KM, Yang C, Krishnakumar R, Kraus WL. The histone variant macroH2A1 marks repressed autosomal chromatin, but protects a subset of its target genes from silencing. Genes Dev. 2010; 24:21-32.
29. Lavigne MD, Vatsellas G, Polyzos A, Mantouvalou E, Sianidis G, Maraziotis I, Agelopoulos M, Thanos D. Composite macroH2A/NRF-1 nucleosomes suppress noise and generate robustness in gene expression. Cell Rep. 2015; 11:1090-1101.
30. Mohammed Ismail W, Mazzone A, Ghiraldini FG, *et al.* MacroH2A histone variants modulate enhancer activity to repress oncogenic programs and cellular reprogramming. Commun Biol. 2023; 6:215.
31. Palozola KC, Donahue G, Liu H, Grant GR, Becker JS, Cote A, Yu H, Raj A, Zaret KS. Mitotic transcription and waves of gene reactivation during mitotic exit. Science. 2017; 358:119-122.
32. Bakhoum SF, Cantley LC. The multifaceted role of chromosomal instability in cancer and its microenvironment. Cell. 2018; 174:1347-1360.

Received August 26, 2023; Revised September 14, 2023; Accepted September 24, 2023.

[§]These authors contributed equally to this work.

Address correspondence to:
Xinhui Li, School of Biomedical Engineering, Shanghai Jiao Tong University, Shanghai 200240, China.
E-mail: xhli@sjtu.edu.cn

Zhifeng Shao, State Key Laboratory of Systems Medicine for Cancer, School of Biomedical Engineering, Shanghai Jiao Tong University, Shanghai 200240, China
E-mail: zfshao@sjtu.edu.cn

Released online in J-STAGE as advance publication September 29, 2023.